

# Micromachined Millimetre-Wave Passive Components at 38 and 77 GHz

Yi Wang<sup>(1)</sup>, Maolong Ke<sup>(1)</sup>, Michael J. Lancaster<sup>(1)</sup>, Frederick Huang<sup>(1)</sup>, Rob Lewis<sup>(2)</sup>

<sup>(1)</sup>*School of Electronic, Electrical and Computer Engineering, University of Birmingham, B15 2TT, U.K.*

*Email: y.wang.6@bham.ac.uk*

<sup>(2)</sup>*BAE Systems Advanced Technology Centre, Chelmsford, CM2 8HN, U.K.*

**Abstract:** A precision micro-fabrication technique has been developed for millimetre-wave components of air-filled three-dimensional structures, such as rectangular coaxial lines or waveguides. The devices are formed by bonding several layers of micromachining defined slices with a thickness of a few hundred micrometres. The slices are thick-photoresist SU8 defined by photolithography, or silicon with a pattern defined by deep reactive ion etching; both are coated with gold by evaporation. The process is simple, and low-cost, as compared with conventional precision metal machining, but yields mm-wave components with good performance. The components are light weight and truly air-filled with no dielectric support. This paper reviews several of these micromachined mm-wave components at 38 and 77 GHz for communications and radar applications.

## INTRODUCTION

A well shielded three-dimensional (3D) structure, such as a coaxial line or a waveguide, is often desired for high-performance low-loss devices. This is particularly so, coming to the millimetre wave (mm-wave) region, where the conductors and dielectrics in planar transmission structures present significant losses. Also, the lack of shielding, such as in microstrip, often causes problems with spurious cross-coupling or detrimental parasitic modes, such as the dielectric-related surface waves. A shielded and dielectric-free 3D structure is a good solution to these problems. A good shielding prevents cross-coupling and enables densely packed circuits. Such a 3D structure usually offers lower conductor losses due to a spread in the surface current distribution. The absence of the dielectrics avoids not only any dielectric losses, but also the dielectric-related parasitic modes. Such structures as metallic coaxial cables and waveguides have been widely used for passive components at mm-wave frequencies. However, their high performance is at the cost of large volume occupancy especially for complex circuits and systems. In addition, the shrinkage of the device footprint with the decreasing wavelength usually means an increase in fabrication cost because of the increased precision required.

The development of micromachining techniques offers a new possibility of fabricating such devices with higher precision and possibly at a lower cost [1]. In contrast with the conventional precision machining where devices are often milled from bulk metals, etching-and-multilayer based technique is employed. The device may be made of non-metallic materials, such as silicon or a polymer, and finished by coating with highly-conductive gold or silver. A precision micro-fabrication technique has been developed for air-filled 3D structures [2], such as rectangular coaxial lines [3] (the conventional round coaxial structure is not compatible with the process) or waveguides. The devices are formed by bonding several layers of micromachining defined slices with a thickness of a few hundred micrometres. The slices are either thick-photoresist SU8 [4] defined by photolithography, or silicon with a pattern defined by deep reactive ion etching, both are then coated with gold by evaporation. The SU8 photoresist is a potentially low cost material and capable of producing high aspect ratio structures, while only requiring standard ultraviolet photolithography.

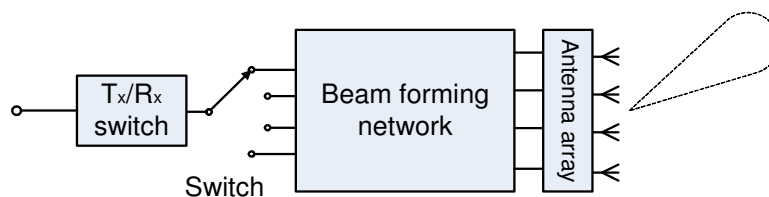


Fig. 1. A transceiver system with switched beam-forming capability.

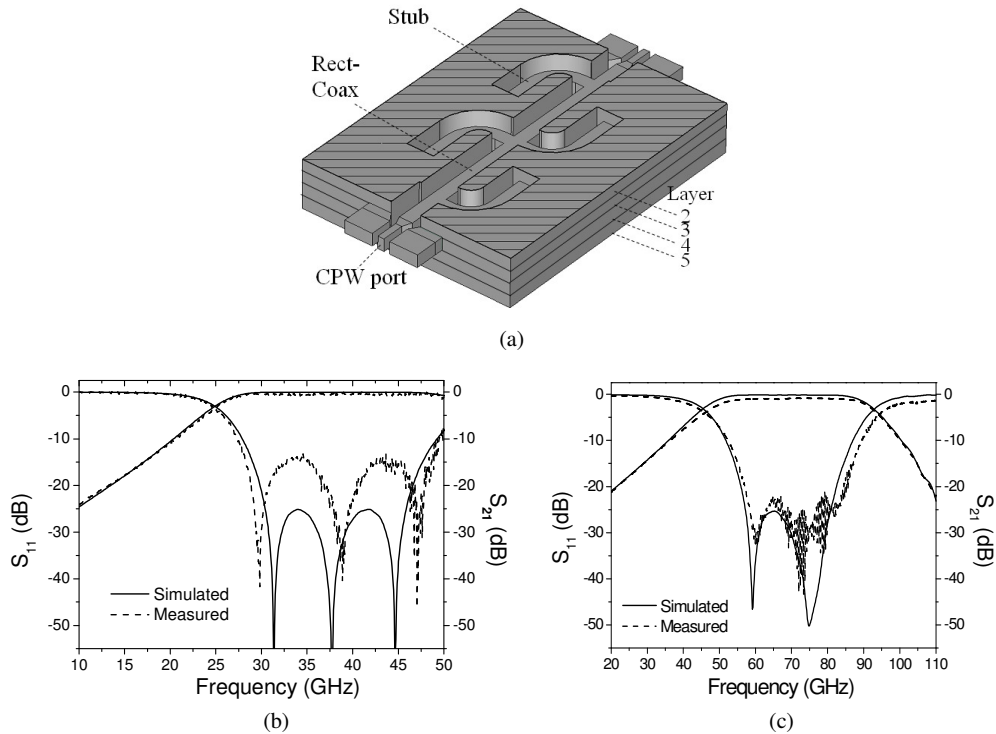


Fig. 2. Rectangular coaxial lines supported by bent stubs: the structure diagram with the top layer removed to assist viewing [8] (a) and the simulated and measured responses for the 38 GHz device (b) and the 77 GHz device (c). All the simulations including those to be mentioned were performed in CST Microwave Studio [5].

Among the possible millimetric applications [6] are imaging radars, high-speed large-volume data transfer, point-to-point wireless communications, and automobile related applications, such as anti-collision radars, and telematics in road networks, etc. This paper reviews several micromachined mm-wave components at 38 and 77 GHz for communications and radar applications. As an exemplary demonstration, a Butler matrix for beam-forming as well as other related passive components are presented. Fig. 1 shows a millimetric transceiver system with switched beam-forming capability. Such a switched beam system [7] is a cost-effective alternative to a continuously steerable system. By switching between the inputs to the network, a set of beams with different angular coverage can be produced. This achieves an increased gain and diversity of the transceiver.

## FABRICATIONS

Two different fabrication techniques have been utilized to produce the millimeter-wave components. One is the silicon based deep reactive ion etching. The other is the SU8 based thick-photoresist photolithography. Either process has been used to pattern each layer of the multilayer structures on a single 4-inch wafer. The silicon or SU8 layers used here were 300  $\mu\text{m}$  thick for the 38 GHz devices, and 200  $\mu\text{m}$  thick for the 77 GHz devices. As required, the silicon layer could be 0.5 mm thick, and the SU8 layer could be as thick as 2 mm [8]. The patterned layers, including all side walls, were then coated with a 20 nm chrome adhesion layer and 2  $\mu\text{m}$  gold or a mixture of silver and gold. These metalized layers were bonded together on top of each other to form the 3D enclosed structures.

## DESIGNS AND IMPLEMENTATION

### Stub-supported Rectangular Coaxial Lines

A building block of any rectangular coaxial based component and system is the rectangular coaxial line. Due to the air-filled nature of the rectangular coaxial structure, the central conductor has to be supported without using any dielectric materials. This has been achieved through short circuited stubs, which are about a quarter of a wavelength long and

placed at appropriate separations. Such a limited but wide bandwidth ‘line’ can be designed as a stub supported filter [9]. Shown in Fig. 2(a) is such a stub-supported rectangular coaxial line [10], 7.6 mm × 3.0 mm × 1.5 mm in size, and covering the frequency range from 28 to 48 GHz. The measured responses are shown in Fig. 2(b). An average insertion loss of 0.36 dB, or 0.048 dB/mm, and a return loss of 14 dB has been achieved. A similar structure to cover 55 to 87 GHz gave responses as shown in Fig. 2(c) [11]. The attenuation is 0.21 dB/mm at 70 GHz and its size is 3.9 mm × 2.0 mm × 1.0 mm. The insertion losses of these two coaxial lines are still higher than predicted due to the imperfections in fabrication, such as the gaps and misalignment between the bonding layers, and the lower than expected conductivity of the coating. In Fig. 2(a), the stubs are bent to minimize the footprint. To facilitate the measurements using on-wafer probes, transitions are made from the rectangular coaxial line to air-filled coplanar waveguide at the input and output ports.

### Rectangular Coaxial Branch-line Couplers

A hybrid branch-line coupler is an important component widely used in many signal distribution devices and systems. This can be realized using a rectangular coaxial structure, as shown in Fig. 3(a) [12]. The quarter wavelength stubs in this branch-line coupler are primarily used to suspend the central conductor of the coaxial line. It has been found that properly placing them enhances the bandwidth of the otherwise narrow-band branch-line couplers. A bandwidth of 33 % can be obtained, as opposed to a typical bandwidth of about 18% for a conventional branch-line coupler. The size of the coupler is 8.3 mm by 7.9 mm in area and 1.5 mm in height. Fig. 3(b) shows the measured results in comparison with simulations. The output through the coupled and through port is 3.2-4.0 dB between 31.3 and 47.6 GHz. Ideally this should be 3 dB for a lossless device. The isolation is better than 12.8 dB, and the return loss less than -15 dB.

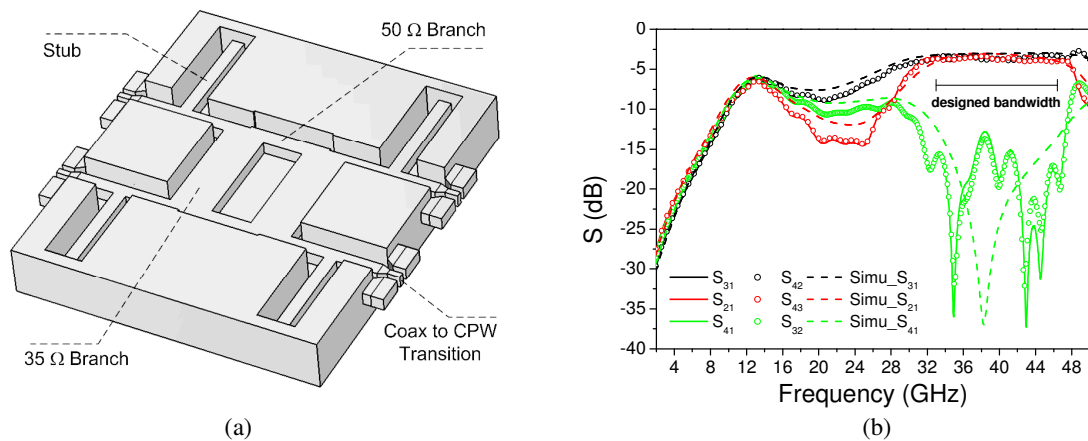


Fig. 3. The branch-line coupler: the diagram with the top layer removed to assist viewing (a), and the simulated and measured responses (b).

### Rectangular Coaxial Line Butler Matrix with Antenna Arrays

Built on the branch-line couplers, a more complex network can be formed from the rectangular coaxial structure. Shown in Fig. 4 is a complete Butler matrix used for switching the beam of a four-element antenna array at 38 GHz [13]. The device occupies a footprint of 26 mm by 23 mm with a height of 1.5mm. According to simulations [10], the Butler matrix has return losses less than -16 dB and inter-port isolations below -22 dB. The output is 6.5±0.3 dB for an input at Port-1 and 6.6±0.5 dB for an input at Port-2. Ideally these should be 6 dB in a lossless case. The radiating element is an air-filled micromachined patch antenna and 3.27 mm by 3.54 mm in size. Removing the dielectric avoids not only the dielectric loss, but also parasitic surface-waves that often exist in substrate-supported mm-wave antennas. The simulated gain of the single patch is 9.4 dBi. Its efficiency is 96 % based on an assumed conductivity of  $2.45 \times 10^7$  S/m, which is 60% that of gold. This value of gain is very high for a single element. The gain measurement is not yet available to confirm the simulation. It is likely that the feed to the patch and the surrounding structures also contribute to the radiation. The four-element array would give a maximum gain of 13 dBi according to simulations. The beam angles are -42.5°, -13°, +13°, and +42.5° respectively. These agree reasonably well with an ideal array, with angles of -48.6°, -14.5°, 14.5° and 48.6°. Fig. 5 shows the simulated beam pattern of the Butler matrix fed antenna array. The

measurement of one beam is also shown. These are still preliminary results from a free-space probe-based radiation measurement. The ripple in the pattern is believed to be a result of insufficient shielding of the measurement probes and is currently being improved.

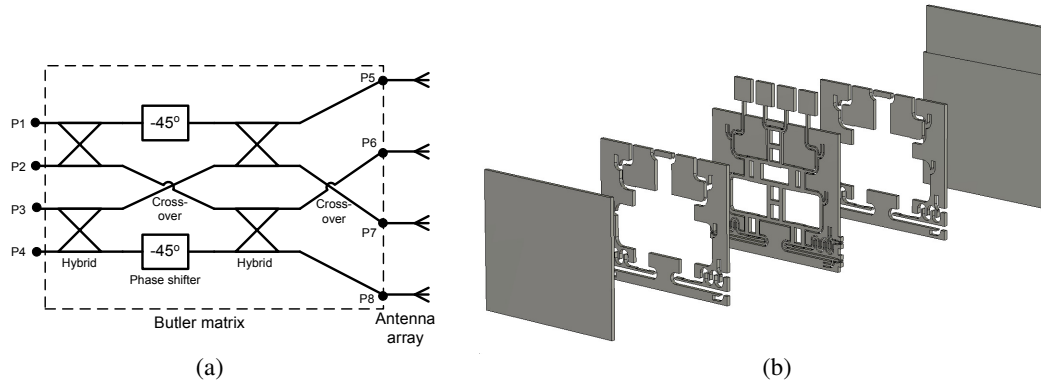


Fig. 4. The schematic diagram (a) and the exploded layout (b) of a 4x4 Butler matrix with antenna array [12].

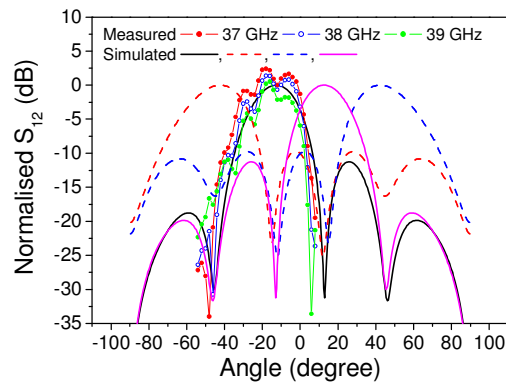


Fig. 5. The simulated beam patterns of the Butler matrix fed antenna array. Also shown is the measurement for one beam.

### Cavity Filters and Resonators

Another miniaturized 3D transmission structure that can be fabricated using the multilayered process is a waveguide. A two-pole waveguide cavity filter [14] has been demonstrated as shown in Fig. 6. The resonator is a reduced-height  $TE_{101}$  mode cavity. The feed line is an integrated rectangular coaxial line. The filter achieved a bandwidth of 4.2% with a return loss better than -15 dB, and an insertion loss of 1 dB at 38 GHz. The separately made 38 GHz and 77 GHz resonators gave the resonant unloaded  $Q$ -values of 343 and 569, respectively. It should be noted that a second gold evaporation has been applied before finalizing the device with the top-layer bonded, in order to improve the quality of the inner side-walls. Because of the current concentration on these side-walls for the resonant mode, the reduced bonding gaps and the thickened conductive coating by this extra evaporation greatly decreases the insertion loss of the filter, as indicated by the comparison in Fig. 6(b).

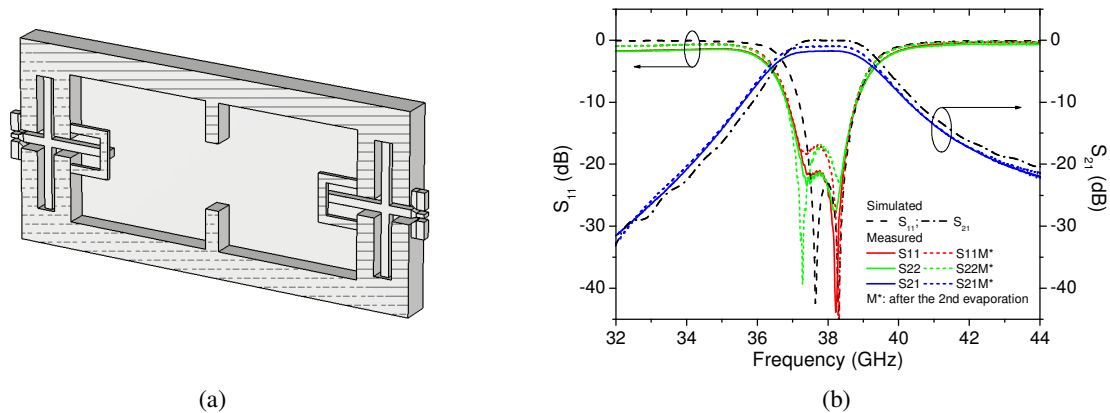


Fig. 6. (a) Diagram of the two-port cavity filter at 38 GHz (The top layer is removed to assist viewing); (b) The measured and simulated responses.

### DISCUSSIONS AND CONCLUSIONS

This micromachining and multilayer bonding technique has been successfully used to produce several working mm-wave components with good performance. Among others being developed are filters, duplexers, and antenna arrays for mm-wave and sub-millimeter wave frequencies. One major advantage of this micromachining process is its relatively simple process, i.e. normally only one etching step (either deep reactive etching or ultraviolet photolithography) is required to produce the air-filled 3D structures. Miniaturized and complex structures, requiring more design effort, would not necessarily increase the fabrication difficulty, whereas with conventional precision machining the production of complex designs is usually time consuming and expensive.

The further integration of the micromachined mm-wave components into a system will require interconnections with the monolithic microwave integrated circuit. This could be done by making transitions to substrate supported coplanar waveguide from the rectangular coaxial ports.

The devices demonstrated here show very competitive performance as compared to similar devices fabricated using various other micromachining techniques [15]-[18]. However, they still cannot match the performance of the larger conventional coaxial or waveguide structures used at these frequencies. This is partly due to the miniaturisation nature of the micromachined devices, which inherently bear more losses. Also, the current micromachining process produces devices which are not up to expectation because of various imperfections in the fabrication. The main factor limiting the achievable performance came from the bonding process for the multiple layers. Although alignment can be tightly controlled, the almost inevitable tiny gaps or unevenness at the bonding interface where currents flow, increase the losses greatly. Whenever possible, as in the cavity filter shown in Fig. 6, a second evaporation has been applied to mitigate these imperfections. Over-etching is another possible error factor that has been identified. This is more of a problem for the silicon deep reactive etching process than the SU8 photolithography. The SU8 process also results in reduced surface roughness on the side walls. Its success largely relies on the quality of the conductive coating and the planarity of each device layer. It has been observed that the conductivity of the gold coating may be 60 % or even less of the value for perfect gold. An improvement on the coating quality is desired.

### ACKNOWLEDGMENTS

This work was funded by UK Engineering and Physical Science Research Council (EPSRC) under EP/D059933/1. The authors would like to thank Prof. P. S. Hall, Dr. P. Gardner, and Dr. K. Jiang, all with the University of Birmingham, U.K., for the helpful discussion.

### REFERENCES

[1] T. M. Weller, L. P. B. Katehi, and G. M. Rebeiz, "High performance microshield line components," *IEEE Trans. Microw. Theory Tech.*, vol. 43, no. 3, pp. 534–543, Mar. 1995.

- [2] M. J. Lancaster, J. Zhou, M. L. Ke, Y. Wang, and K. Jiang, "The design and high performance of a Micromachined K-band rectangular coaxial cable", *IEEE Trans Microwave Theory Tech.*, vol. 55, pp.1548–1553, 2007.
- [3] T. S. Chen, "Determination of the capacitance, inductance, and characteristic impedance of rectangular lines", *IRE Trans. Microwave Theo. Tech.*, vol. 8, no. 5, pp.510-519, Sept. 1960.
- [4] R. Yang and W. Wang, "A numerical and experimental study on gap compensation and wavelength selection in UV-lithography of ultrahigh aspect ratio SU-8 microstructures," *Sens. Actuators B, Chem.*, vol. 110, no. 2, pp. 279–288, Oct. 2005.
- [5] CST Microwave Studio, CST GmbH, Germany 2006.
- [6] W. Menzel, "50 years of millimetre-waves: a journey of development", *Microwave J.*, vol. 51, no. 8, pp. 28-42, 2008
- [7] P. S. Hall, S. J. Vetterlein, "Review of radio frequency beamforming techniques for scanned and multiple beam antennas", *IEE Proc. H-Microwaves, Antennas and Propagation*, vol. 137, no. 5, pp. 293-303, Oct. 1990.
- [8] J. D. Williams and W. Wang, "Study on the postbaking process and the effects on UV lithography of high aspect ratio SU-8 microstructures," *Journal of Microlithography, Microfabrication, and Microsystems*, vol. 3, pp. 563-568, 2004.
- [9] G. Matthaei, L. Young, and E. M. T. Jones, *Microwave Filters, Impedance-Matching Networks and Coupling Structure*, Norwood, MA: Artech House, 1980.
- [10] M. Ke, Y. Wang, M. J. Lancaster, "Design and realisation of low loss air-filled rectangular coaxial cable with bent quarter-wavelength supporting stubs", *Microwave and Optical Technology Letters*, vol. 50, pp. 1443-1446, May 2008.
- [11] M. Ke, Y. Wang, M. J. Lancaster, "Micromachined Rectangular Coaxial Line and Cavity Resonator for 77 GHz Applications using SU8 Photoresist", *Asia Pacific Microwave Conference 2008*, Hong Kong.
- [12] Y. Wang, M. Ke, M. J. Lancaster, F. Huang, "Micromachined Millimeter-wave Rectangular-Coaxial Branch-Line Couplers with Enhanced Bandwidth", *IEEE Trans. Microw. Theory Tech.*, in press.
- [13] Y. Wang, M. Ke, M. J. Lancaster, "A Ka-Band Butler Matrix with Antenna Array Based on Micromachined Rectangular Coaxial Structures", submitted to *European Microwave Conference 2009*, unpublished.
- [14] Y. Wang, M. Ke, M. J. Lancaster, "Micromachined 38GHz Cavity Resonator and Filter with Rectangular-Coaxial Feed-lines", *IET Microwaves, Antennas & Propagation*, vol. 3, no. 1, pp. 125-129, Feb. 2009.
- [15] R. T. Chen, E. R. Brown, and C. A. Bang, "A compact low-loss Ka-band filter using 3-dimensional micromachined integrated coax," in *17th IEEE Int. MEMS Conf.*, Maastricht, The Netherlands, pp. 801–804, Jan. 2004.
- [16] I. Jeong, S.-H. Shin, J.-H. Go, J.-S. Lee, C.-M. Nam, D.-W. Kim, and Y.-S. Kwon, "High-performance air-gap transmission lines and inductors for millimeter-wave applications," *IEEE Trans. Microw. Theory Tech.*, vol. 50, no. 12, pp. 2850–2855, Dec. 2002.
- [17] M. Stickel, P. Kremer, G. V. Eleftheriades, "A millimeter-wave bandpass waveguide filter using a width-stacked silicon bulk micromachining approach", *IEEE Microw. Wirel. Compon. Lett.*, 16, (4), pp. 206–211, 2006.
- [18] K. Vanhille, D. Filipovic, C. Nichols, D. Fontaine, "Balanced Low-Loss Ka-Band  $\mu$ -Coaxial Hybrids," in *2007 IEEE MTT-S Int. Microwave Symp. Dig.*, pp. 1157-1160, Jun. 2007.